ВЫСШАЯ ШКОЛА ЭКОНОМИКИ
НАЦИОНАЛЬНЫЙ ИССЛЕДОВАТЕЛЬСКИЙ УНИВЕРСИТЕТ

Quantum acoustics

Доклад по статье M. Biled, et al, "Schrödinger cat states of a 16-microgram mechanical oscillator", Science 380, 274–278 (2023)

А.М.Сатанин
профессор МИЭМ НИУ ВШЭ,
ВНС лаборатории вычислительной физики

Outline

- **Introduction**
- **Nonclassical states**
- **Quantum superposition, entanglement and Schrödinger's cat paradox**
- **Quantum acoustics**
- **Resonators, phonons and qubits**
- **Quantum acoustics**
- **Wigner function**
- **Jaynes-Cummings model**
- **M. Biled, et al, "Schrödinger cat states of a 16-microgram mechanical oscillator",**
- **Summary**

Nonclassical states like superposition and entanglement

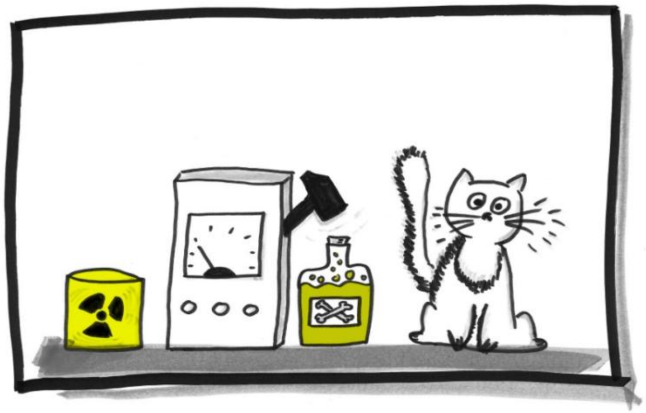

From Julian Göttsch

E. Schrödinger, Die gegenwärtige Situation in der Quantenmechanik. Naturwissenschaften 23, 807–812 (1935)
can be found, in an English translation, in Quantum Theory of Measurement, edited by J. A. Wheeler and W. H. Zurek (Princeton: Princeton University Press, 1983), pp. 152–167

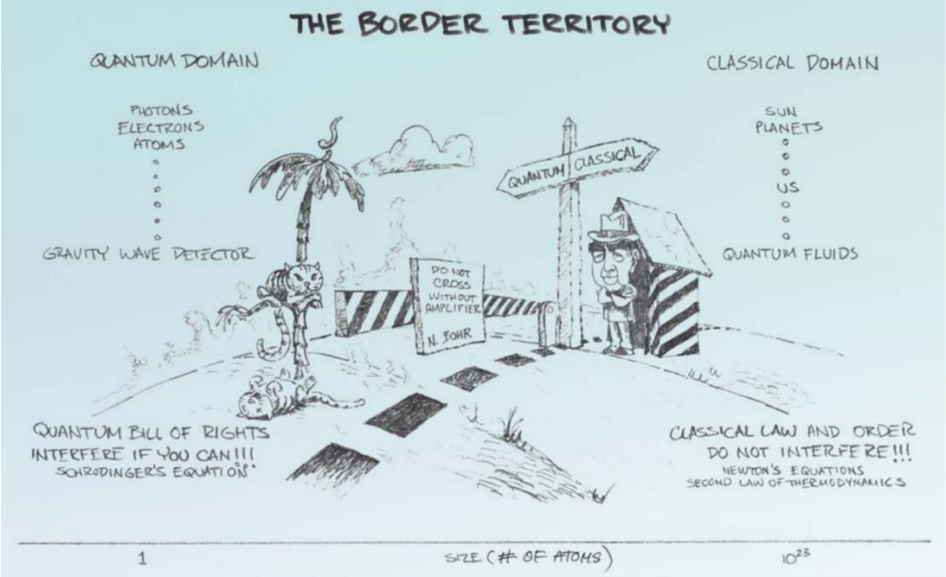

Quantum superposition

$$|\psi\rangle = c_1|\psi_1\rangle + c_2|\psi_2\rangle + \cdots$$

Phthalocyanine is a large, aromatic, macrocyclic, organic compound with the formula $(C_8H_4N_2)_4H_2$

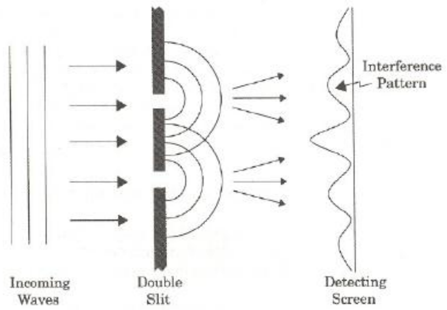

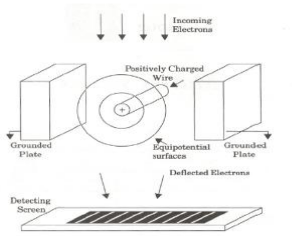

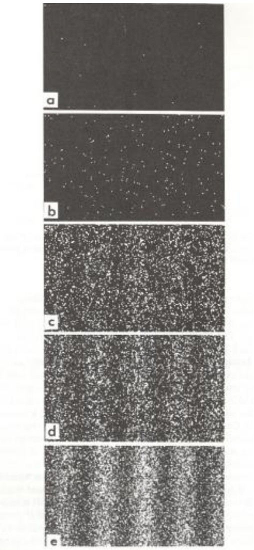

A.Tonomura, Am.J.Phys.57,117(1989)

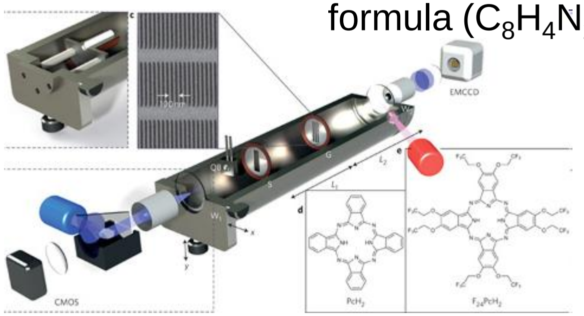

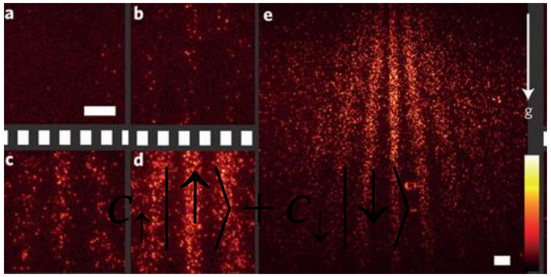

University of Vienna, Thomas Juffmann et al./Nature Nanotechnolog

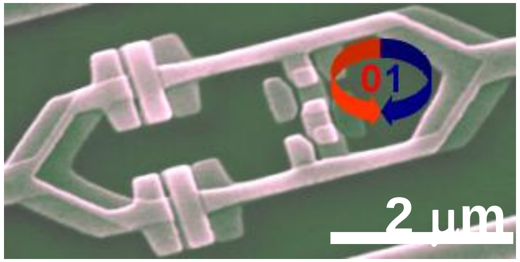

Mooij *et al.*, Science 285, 1036, 1999

flux qubit/Delft

Entanglement

Entanglement is a term used in quntum theory to describe the way that particles of energy/matter can become ***correlated*** to predictably interact with each other regardless of how far apart they are. E. Schrödinger, Naturwissenschaften 23, 807 (1935).

Interaction

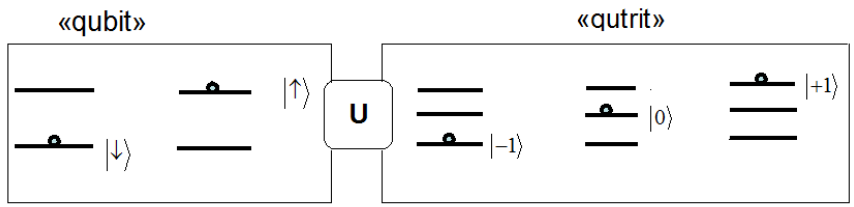

$\mathbf{U}|\uparrow,0\rangle = |\uparrow,+1\rangle$

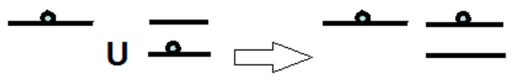

$$c_\uparrow|\uparrow\rangle + c_\downarrow|\downarrow\rangle$$

$\mathbf{U}\ |\downarrow,0\rangle = |\downarrow,-1\rangle$

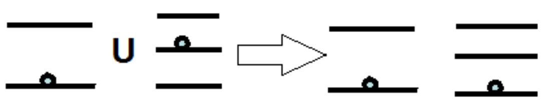

An initial state of the decoupled system:

$$\left(c_\uparrow|\uparrow\rangle + c_\downarrow|\downarrow\rangle\right)\otimes|0\rangle = c_\uparrow|\uparrow,0\rangle + c_\downarrow|\downarrow,0\rangle$$

Entanglement:

$$U\left(c_\uparrow|\uparrow,0\rangle + c_\downarrow|\downarrow,0\rangle\right) = c_\uparrow|\uparrow,+1\rangle + c_\downarrow|\downarrow,-1\rangle$$

A maximal entangled state: $c_\uparrow = -c_\downarrow$

$$|s\rangle = \frac{1}{\sqrt{2}}\left(|\uparrow,+1\rangle - |\downarrow,-1\rangle\right)$$

How to prepare entangled states of photons in the microwave frequency domain?

Selected for a Viewpoint in *Physics*
PRL **112**, 170501 (2014) PHYSICAL REVIEW LETTERS week ending 2 MAY 2014

Observation of Measurement-Induced Entanglement and Quantum Trajectories of Remote Superconducting Qubits

N. Roch,[1,*] M. E. Schwartz,[1] F. Motzoi,[2] C. Macklin,[1] R. Vijay,[3] A. W. Eddins,[1] A. N. Korotkov,[4] K. B. Whaley,[2] M. Sarovar,[5] and I. Siddiqi[1]

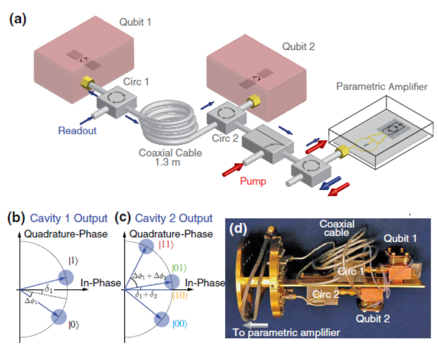

FIG. 1 (color online). Experimental setup. (a) Simplified representation of the experimental setup. (b) and (c) Schematic of the phase shift acquired by a coherent state sequentially measuring first qubit 1 (b) and then qubit 2 (c) in reflection. (d) Picture of the base-temperature setup.

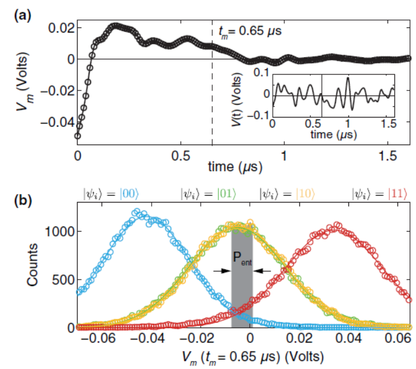

FIG. 2 (color online). Demonstration of indistinguishability between $|01\rangle$ and $|10\rangle$ computational states during measurement. (a) Example of the temporal evolution of the measurement signal V_m. The inset shows the associated instantaneous voltage $V(t)$.

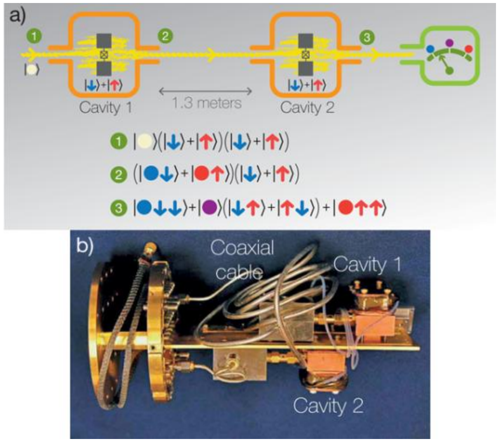

Entanglement between distant macroscopic mechanical and spin systems

Rodrigo A. Thomas et al. Nature Physics | www.nature.com/naturephysics (2020)

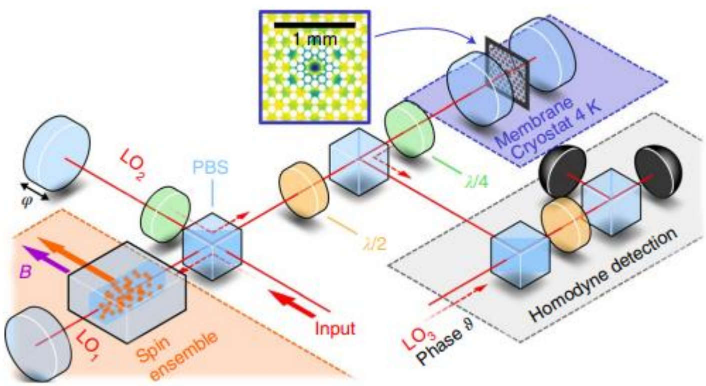

We generate an entangled state between the motion of a macroscopic mechanical oscillator and a collective atomic spin oscillator, as witnessed by an Einstein–Podolsky– Rosen variance below the separability limit, 0.83 ± 0.02 < 1. The mechanical oscillator is a millimetre-size dielectric membrane and the spin oscillator is an ensemble of 109 atoms in a magnetic field.

Experimental investigation of Schrödinger's cat paradox

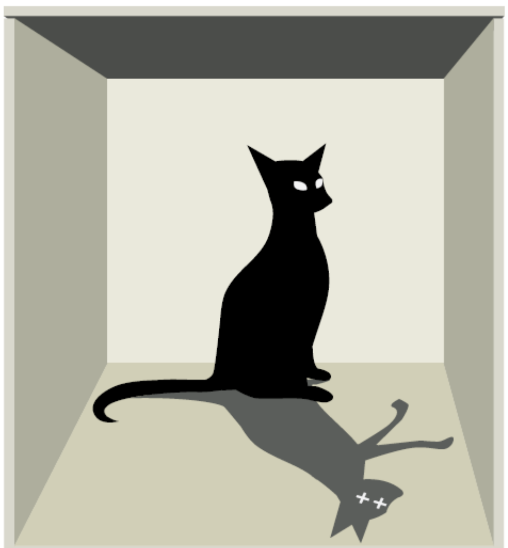

$$|\alpha\rangle$$

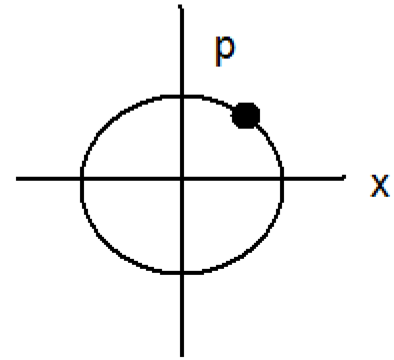

$$H_{osc} = \hbar\omega_0 a^+ a + f_0 \cos\omega t (a + a^+)$$

$$|\alpha(t)\rangle = e^{\alpha(t)a^+ - \alpha^*(t)a} |0\rangle, \quad \frac{d\alpha(t)}{dt} = i f_0 \cos(\omega t)$$

$$\Omega(t) = f_0 \cos(\omega t)$$

The Schrödinger's cat.

$$\left|\alpha e^{-i\omega_0 t}\right\rangle$$

$|\alpha| \ll 1$ → $|\alpha| \gg 1$

Quantum acoustics

Chu et al., Quantum acoustics with superconducting qubits, Science 358, 199–202 (2017)

Here, we experimentally demonstrate a high-frequency bulk acoustic wave resonator that is strongly coupled to a superconducting qubit using piezoelectric transduction with a cooperativity of 260. We measure qubit and mechanical coherence times on the order of 10 microseconds

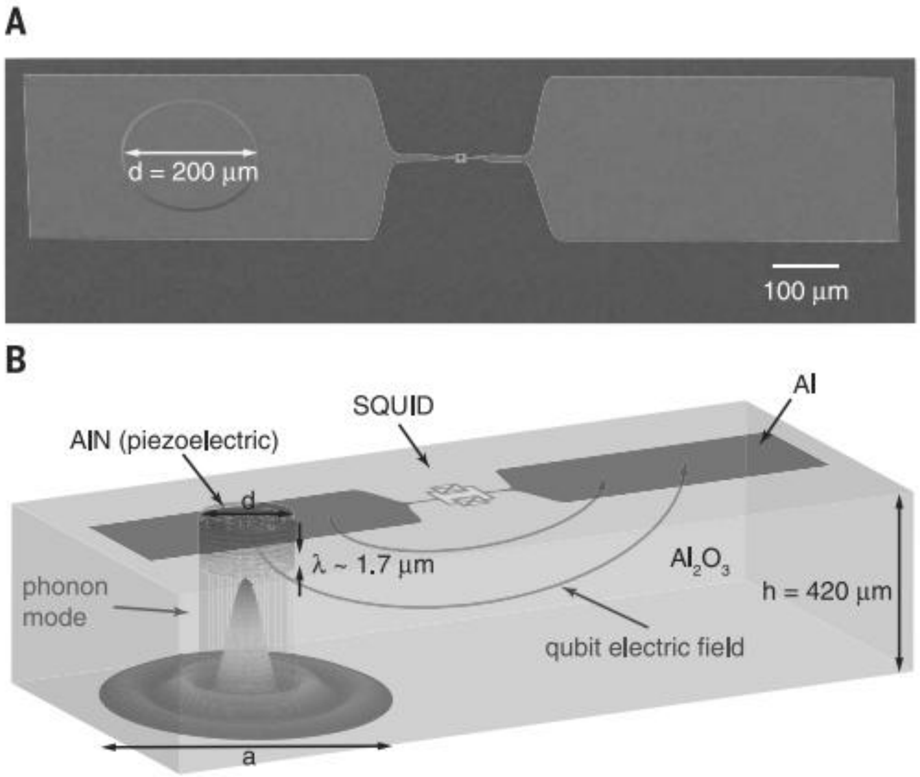

Qubit with piezoelectric transducer

Our quantum electromechanical device, shown in Fig. 1A, consists of a frequency-tunable aluminum transmon coupled to phonons in its nonpiezoelectric sapphire substrate using a thin disk of c-axis–oriented aluminum nitride (AlN)

Phonons

The concept of phonons was introduced in 1932 by Soviet physicist Igor Tamm.

Lattice displacement and effective mass

A Laguerre-Gaussian (LG) mode

$$LG_{pl}(r,\phi) = \sqrt{\frac{2p!}{\pi(p+|l|)!}} \left(\frac{r\sqrt{2}}{w_0}\right)^{|l|} e^{-(r/w_0)^2} L_p^{|l|}\left(\frac{2r^2}{w_0^2}\right) e^{-il\phi} \,,$$

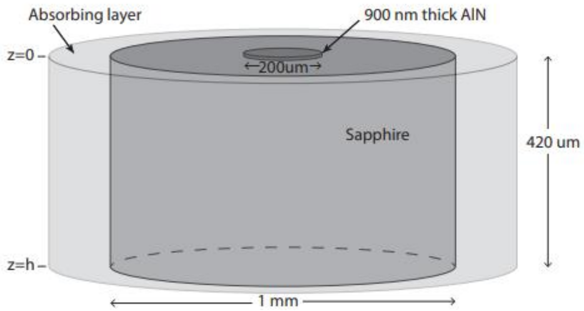

$$s_{plm}(r,\phi,z) = S\, LG_{pl}(r,\phi)\, \sin\left(\frac{m\pi}{L}z\right)$$

$$H/\hbar = \omega_{\text{phonon}} a^\dagger a$$

Transmon qubit

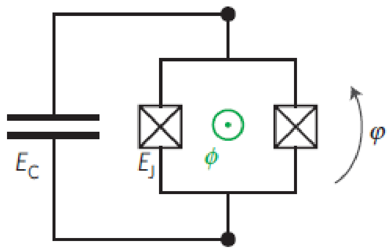

$$100\times 100\ \ nm^2$$

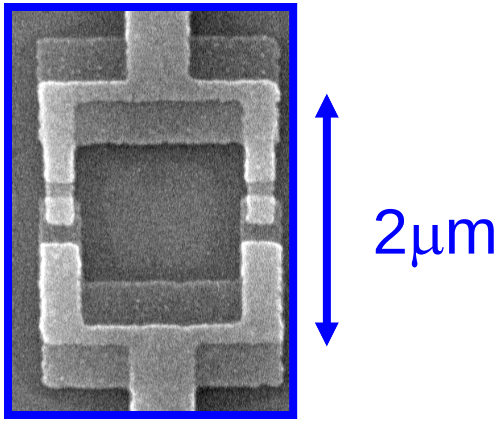

C=10 *p*F $L_J = \Phi_0 / I_c$ $L_J \approx 1\ nH$

$$T \approx 10\ mK$$

$$\frac{\omega_J}{2\pi} = \frac{1}{2\pi}\sqrt{\frac{2eI_c}{\mathrm{h}C}} = \frac{1}{2\pi\sqrt{L_J C}} \approx 1 GHz$$

T=24 mK=500 MHz

$$k_B T << \hbar\omega_J \qquad Q >> 1$$

$$H = 4E_c(\hat{n} - n_g)^2 - E_J \cos\phi$$

Управление состояниями в сверхпроводниковых квантовых процессорах, Вожаков В А, Бастракова М В, Кленов Н В, Соловьев И И, Погосов В В, Бабухин Д В, Жуков А А, **Сатанин А М** *УФН* **192** 457–476 (2022)

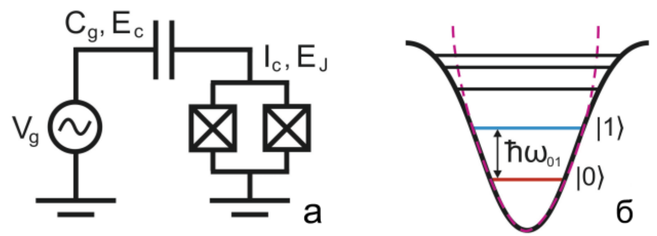

Схематичное изображение трансмона (а) и его потенциальной энергии вместе со спектром энергий стационарных состояний (б).

$$\hat{H} = \omega_{01}\hat{a}^{\dagger}\hat{a} + \omega_{\alpha}\left(\hat{a} + \hat{a}^{\dagger}\right)^{4} - i\varepsilon\left(t\right)\left(\hat{a} - \hat{a}^{\dagger}\right), \tag{4}$$

где $\varepsilon\left(t\right)$ – огибающая для действующего поля, $\omega_{01} = \sqrt{8E_J E_C}/\hbar$, $\omega_{\alpha} = -E_C/12\hbar$.

При условии сильного ангармонизма $E_C \ll E_J$ гамильтониан кубита может быть записан в двумерном фоковском подпространстве $|0\rangle$ и $|1\rangle$, где $\hat{a}^{\dagger}\hat{a}\,|n\rangle = n\,|n\rangle$, что удобно представить через матрицы Паули σ_x, σ_y и σ_z:

$$H = \omega_{01}\sigma_z + \varepsilon\left(t\right)\left(\sigma_x + \sigma_y\right). \tag{5}$$

В качестве базисных состояний можно выбрать спиноры $|0\rangle = \begin{pmatrix} 1 \\ 0 \end{pmatrix}$ и $|1\rangle = \begin{pmatrix} 0 \\ 1 \end{pmatrix}$, а волновую функцию кубита записать в виде:

$$|\Psi_t\rangle = \alpha(t)\,|0\rangle + \beta(t)\,|1\rangle, \tag{6}$$

где α и β – комплексные коэффициенты, $|\alpha|^2 + |\beta|^2 = 1$.

Управление состояниями в сверхпроводниковых квантовых процессорах, Вожаков В А, Бастракова М В, Кленов Н В, Соловьев И И, Погосов В В, Бабухин Д В, Жуков А А, **Сатанин А М** *УФН* **192** 457–476 (2022)

Coupling

Consider only the dominant tensor components

To find the coupling of these modes to the qubit, we can write the mechanical interaction energy as $H = -\int \sigma(\vec{x})s(\vec{x})\, dV = -\int c_{33}d_{33}(\vec{x})E(\vec{x})s(\vec{x})\, dV$. Here, $\sigma(\vec{x})$ is the stress, $E(\vec{x})$ is the qubit's electric field profile, and c_{33} and d_{33} are the stiffness and piezoelectric tensor components, respectively. For simplicity, we are only considering the dominant tensor components perpendicular to the surface of the substrate. Quantizing the qubit mode as $E(\vec{x})(a + a^\dagger)$ and the phonon mode as $s(\vec{x})(b + b^\dagger)$, we can use the rotating wave approximation to equate this interaction energy to the Jaynes-Cummings Hamiltonian $H_{\text{int}} = -\hbar g(ab^\dagger + a^\dagger b)$.

Then the interaction energy between the transmon and the phonon mode

$$H_{\text{int}} = -\hbar g(ab^\dagger + a^\dagger b).$$

parameter	value	parameter	value
$\omega_{\text{qubit}}/2\pi$	5.9456 GHz	ω_{phonon}	5.9614 GHz
$g_0/2\pi$	258 kHz	$\Delta_{\text{dispersive}}/2\pi$	1.85 MHz
$\gamma_1/2\pi$	19 kHz	$\kappa_1/2\pi$	2.5 kHz
$\gamma_2^{\text{Ramsey}}/2\pi$	24 kHz	$\kappa_2^{\text{Ramsey}}/2\pi$	1.5 kHz
$\gamma_2^{\text{E}}/2\pi$	21 kHz	$\kappa_2^{\text{E}}/2\pi$	1.4 kHz

List of qubit and phonon properties and experimental parameters.

Cavity Quantum Electrodynamics (CQED)

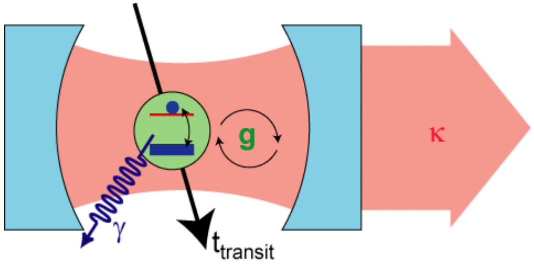

2g = vacuum Rabi freq.

κ = cavity decay rate

γ = “transverse” decay rate

transition dipole vacuum field

Jaynes-Cummings Hamiltonian

$$H = \hbar\omega_r\left(a^\dagger a + \frac{1}{2}\right) + \frac{\hbar\omega_a}{2}\sigma^z + \hbar g(a^\dagger\sigma^- + a\sigma^+) + H_\kappa + H_\gamma$$

strong coupling limit $(g = dE_0/\hbar > \gamma,\ \kappa\,, 1/t_{\mathrm{transit}})$

D. Walls, G. Milburn, Quantum Optics (Spinger-Verlag, Berlin, 1994)

A Circuit Analog for Cavity QED

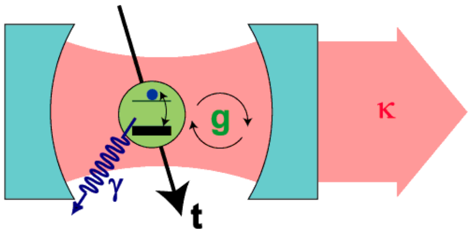

$2g$ = vacuum Rabi freq.

κ = cavity decay rate

γ = “transverse” decay rate

transmission line “cavity”

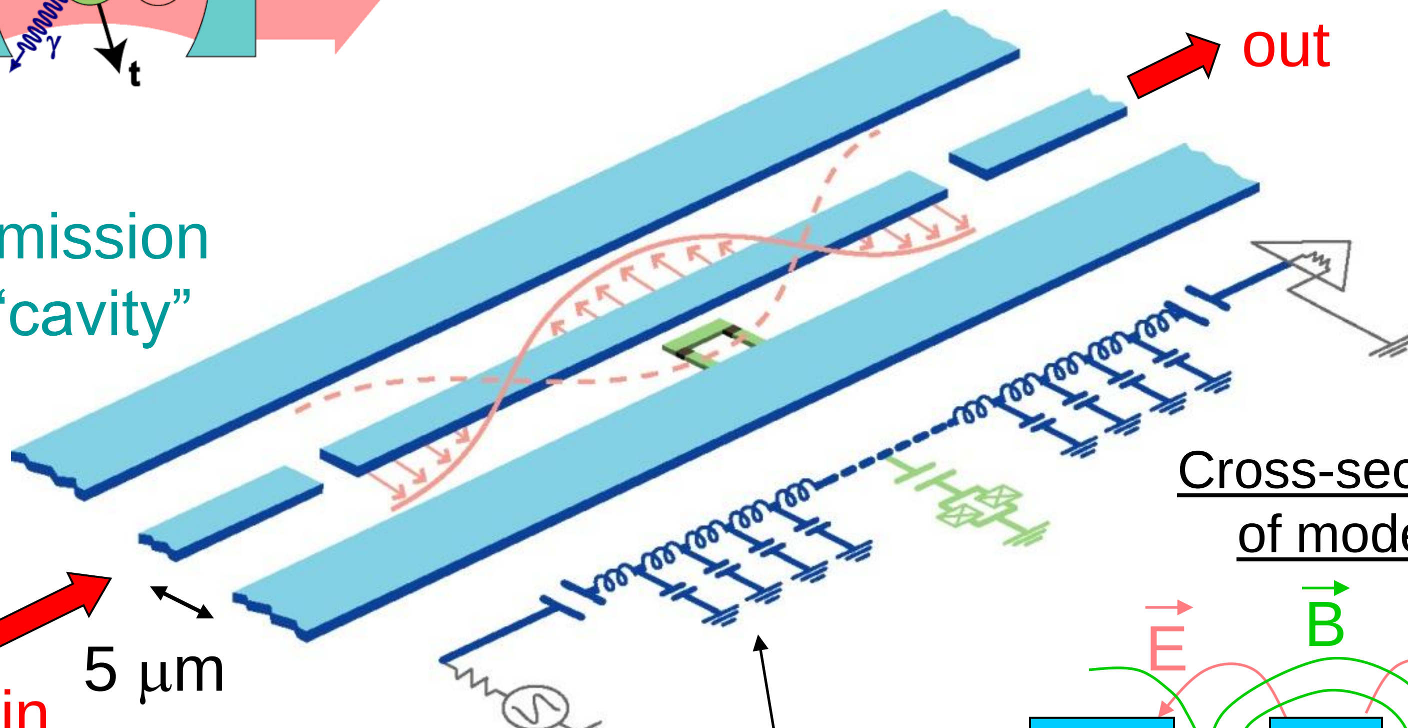

out

DC + 6 GHz in

5 μm

Lumped element equivalent circuit

Cross-section of mode:

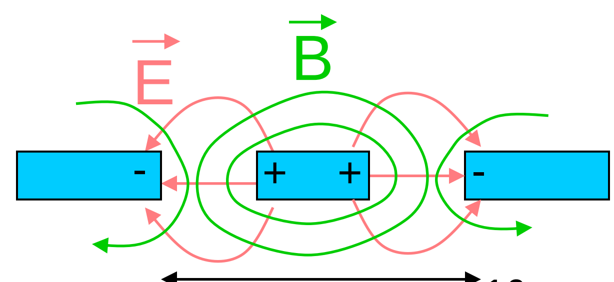

10 μm

Blais, Huang, Wallraff, SMG & RS, PRA 2004

Fock states

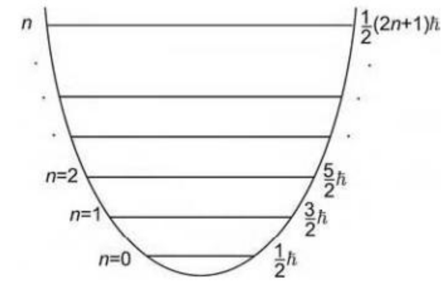

$$\hat{H} = \hbar\omega\hat{a}^{\dagger}\hat{a} \qquad \hat{a}^{\dagger}\hat{a}|n\rangle = n|n\rangle$$

$$|n\rangle = \frac{(\hat{a}^{\dagger})^n}{\sqrt{n!}}|0\rangle$$

$$\langle x|n\rangle = \frac{1}{\sqrt{2^n n!\sqrt{\pi}a}} e^{-x^2/2a} \mathrm{H}_n\left(x/a\right)$$

H. Wang, M. Hofheinz et al, Measurement of the Decay of Fock States in a Superconducting Quantum Circuit, PRL 101 240401 (2008)

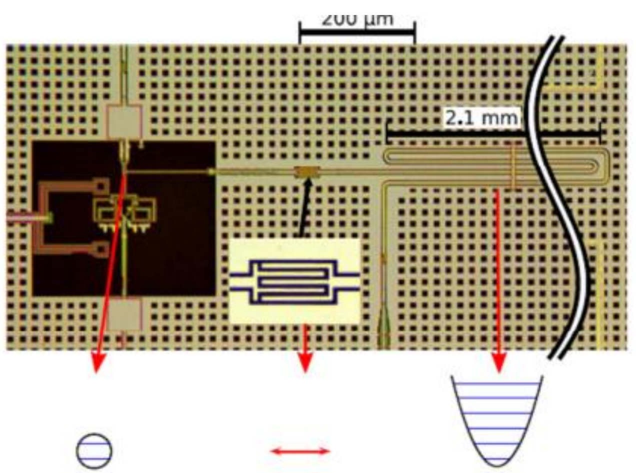

$$H = h\nu_q\sigma^+\sigma^- + \frac{\hbar\Omega}{2}(a\sigma_+ + a^\dagger\sigma_-) + h\nu_r\left(a^\dagger a + \frac{1}{2}\right)$$

кубит

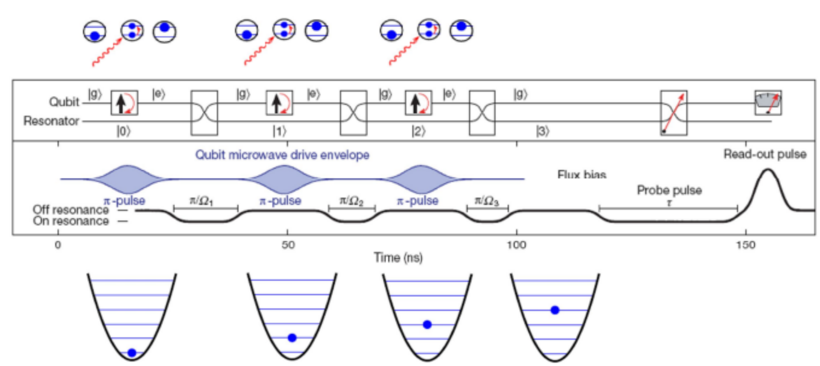

резонатор

Coherent states

$$H = \hbar\omega a^{\dagger} a$$

$$H_{osc} = \hbar\omega_0 a^{+} a + f_0 \cos\Omega t (a + a^{+})$$

$$\hat{a}|\alpha\rangle = \alpha|\alpha\rangle$$

$$\alpha(t) = e^{i\omega(t-t_0)}\alpha(t_0)$$

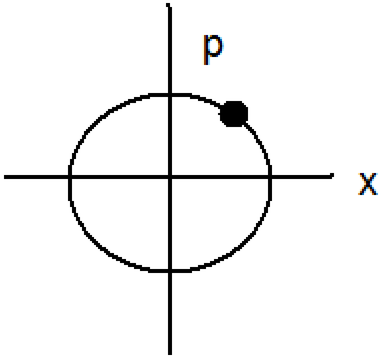

$$D(\alpha) = \exp\left(\alpha a^{\dagger} - \alpha^{*} a\right)$$

$$|\alpha>= D(\alpha)|0>$$

$$|\alpha\rangle = \sum_{n=0}^{\infty} C_n |n\rangle$$

$$|\alpha\rangle = \exp\left(-\frac{1}{2}|\alpha|^2\right)\sum_n \frac{\alpha^n}{\sqrt{n!}}|n\rangle$$

$$|\alpha(t)\rangle = e^{\alpha(t)a^{+} - \alpha^{*}(t)a}|0\rangle, \quad \frac{d\alpha(t)}{dt} = if_0\cos(\omega t)$$

$$\bar{n} = \langle\alpha|\,\hat{a}^{\dagger}\hat{a}\,|\alpha\rangle$$

Coherent states are the most “classical” available in quantum physics, and we will call a Schrodinger cat state a quantum ¨ superposition of coherent states, well separated in phase space

$$S(\xi) = \exp\left(-\frac{1}{2}\left(\xi a^{\dagger 2} - \xi^{*} a^{2}\right)\right)$$

$$|\xi>= S(\xi)|0>$$

$$|\eta\rangle = \frac{1}{\sqrt{\cosh(r)}}\sum_n [(e^{i\theta}/2)\tanh(r)]^n \frac{\sqrt{(2n)!}}{n!}|2n\rangle$$

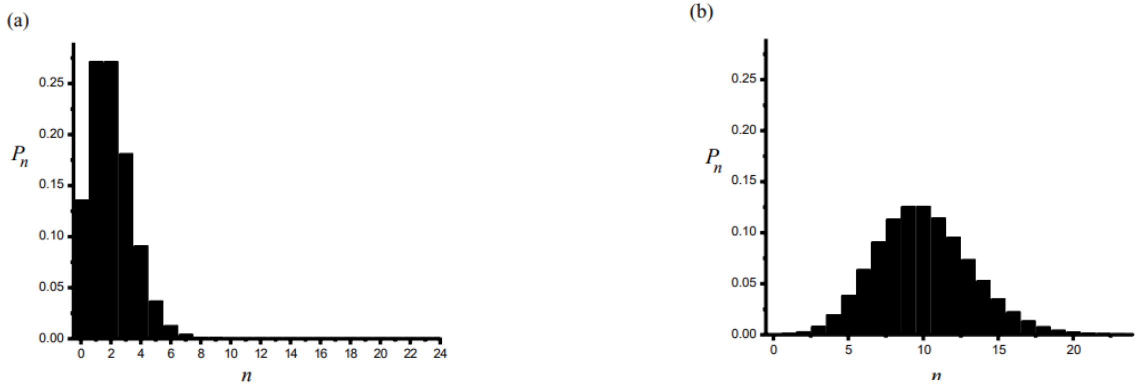

Fig. 3.1. Coherent state photon number probability distributions for (a) $\bar{n} = 2$ and (b) $\bar{n} = 10$.

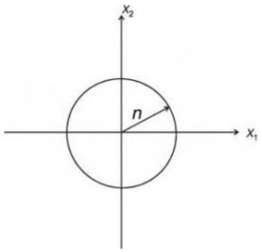

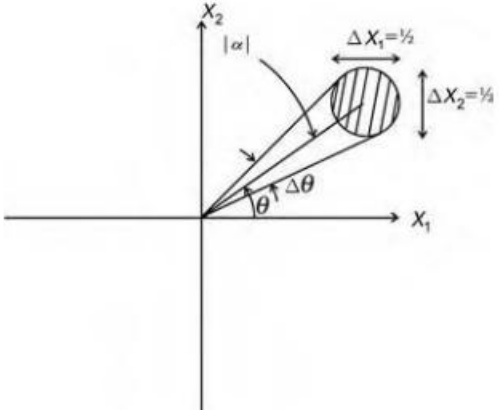

Introductory Quantum Optics by C.Gerry & Knight

Wigner function

E. Wigner, Phys. Rev. 40 749 (1932)

$$W(x,p;t)=\frac{1}{2\pi}\int d\xi e^{-ip\xi}\left\langle x+\frac{1}{2}\xi\middle|\rho(t)\middle|x-\frac{1}{2}\xi\right\rangle$$

$$\hat{p}=\frac{a-a^{+}}{i\sqrt{2}} \qquad \hat{x}=\frac{a+a^{+}}{\sqrt{2}}$$

$$H=\omega_p\hat{a}^{+}\hat{a}+\tilde{f}(t)(\hat{a}+\hat{a}^{+}),\ f(t)=f_0\cos(\Omega t)$$

$$\langle x|n\rangle=\frac{1}{\sqrt{2^n n!\sqrt{\pi}a}}e^{-x^2/2a}\mathrm{H}_n\left(x/a\right)$$

$$\boxed{\frac{\partial\rho}{\partial t}=\frac{1}{i\hbar}[H,\rho]+\frac{\gamma}{2}(2a\rho a^{+}-a^{+}a\rho-\rho a^{+}a)}$$

$$W(x,p;t)=\frac{1}{2\pi}\sum_{n,m=0}^{\infty}\int d\xi e^{-ip\xi}C_n(t)C_m^{*}(t)\left\langle x+\frac{1}{2}\xi\middle|n\right\rangle\left\langle m\middle|x-\frac{1}{2}\xi\right\rangle$$

Quantum Homodyne Tomography

L. G. Lutterbach, L. Davidovich, PRL 78 2547 (1997)

Conventional homodyne detection

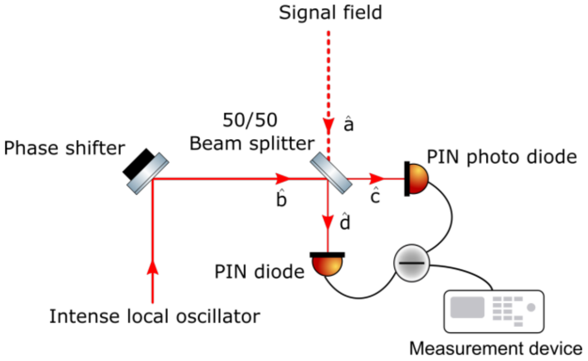

$$w_{\hat\rho}(q) \equiv \frac{1}{\sqrt{2\pi\hbar}} \int dp\, W_{\hat\rho}(q,p) = \sqrt{2\pi\hbar}\langle q|\hat\rho|q\rangle$$

$$\hat{x}_\theta = \sqrt{\frac{\hbar}{2}}\left[\hat{a}e^{-i\theta} + \hat{a}^\dagger e^{i\theta}\right]$$

$$W_{\hat\rho}(q,p) = \frac{1}{(2\pi\hbar)^{3/2}} \int_{-\infty}^{\infty} dx_\theta \int_{-\infty}^{\infty} d\xi\, |\xi| \times \int_0^\pi d\theta\, w_{\hat\rho}(x_\theta,\theta) \exp\left[\frac{i}{\hbar}\xi(x_\theta - q\cos\theta - p\sin\theta)\right]$$

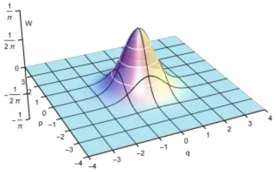

$|0\rangle$

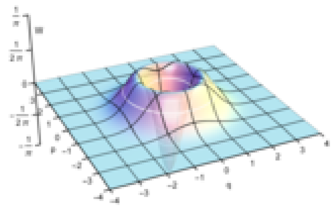

$|1\rangle$

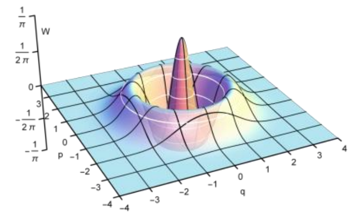

$|2\rangle$

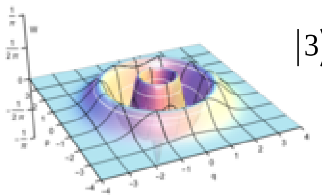

$|3\rangle$

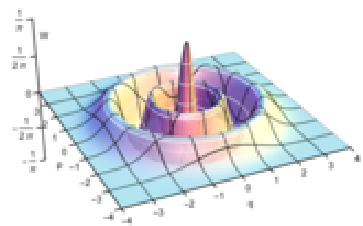

$|4\rangle$

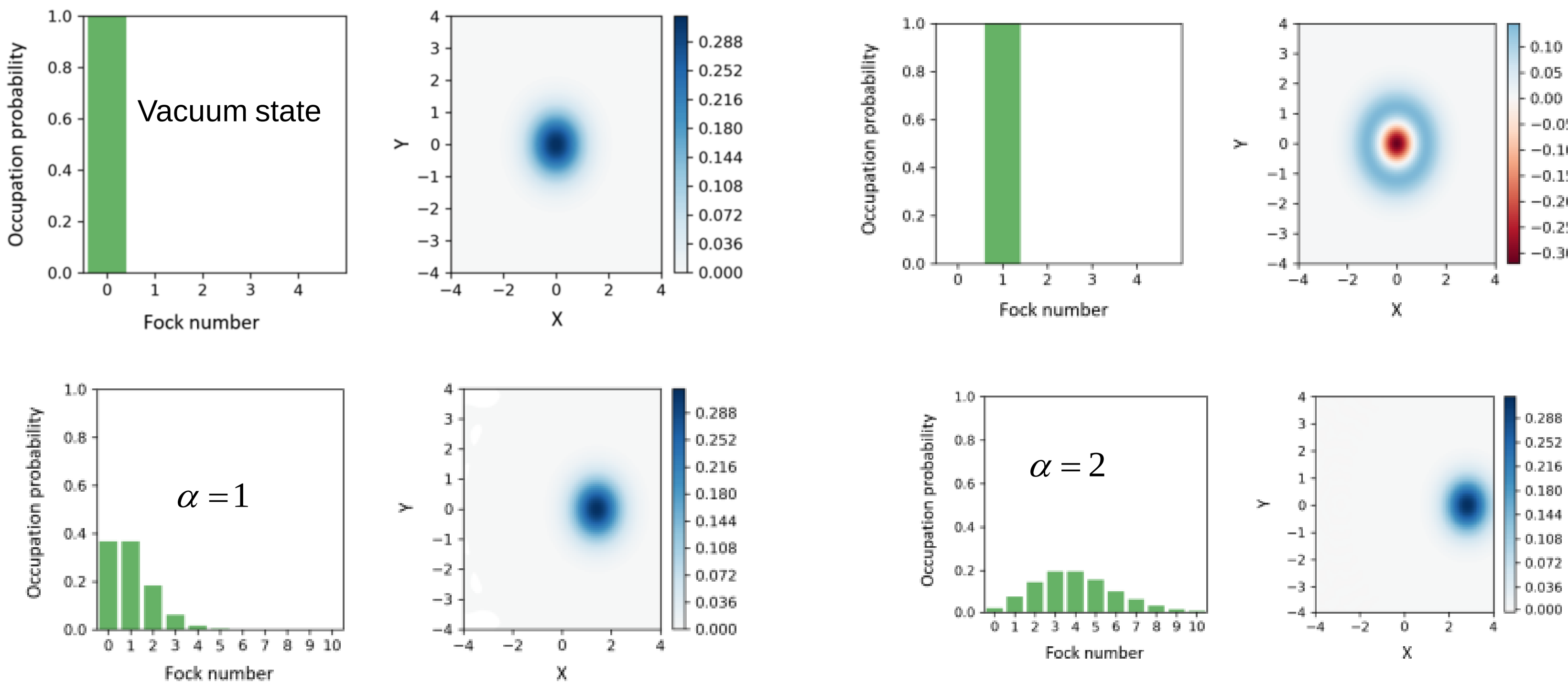

$$W_{|n\rangle}(X,Y) = \frac{1}{\pi} e^{(-X^2-Y^2)} (-1)^n L_n^{(0)} [2(X^2+Y^2)]$$

C. Gerry and P. Knight. Introductory Quantum Optics. Campridge Univ. Press, 2005.

Schrödinger cat state

$$\psi_{cat} \propto \left(|\alpha\rangle \pm |-\alpha\rangle \right).$$

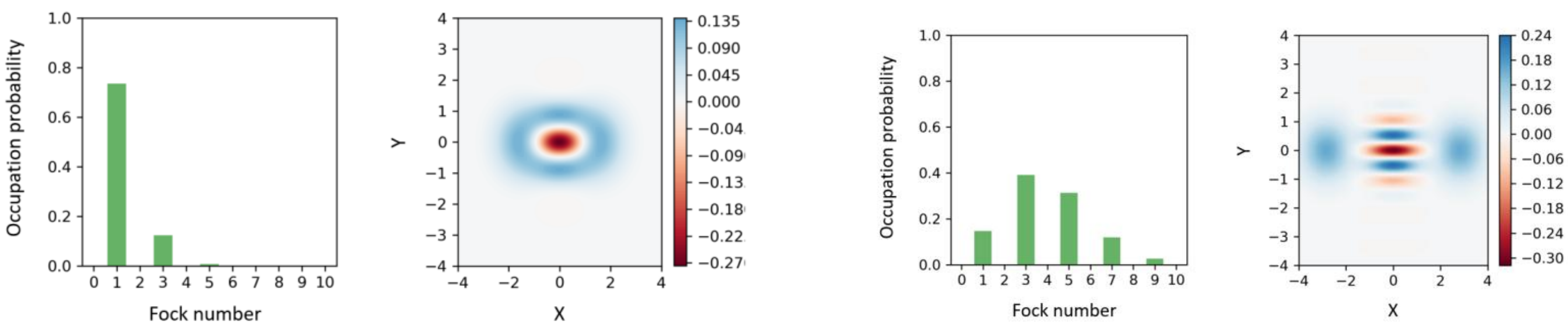

$$\psi_{cat,odd} \propto e^{\frac{-|\alpha|^2}{2}} \sum_{n=0}^{\infty} \frac{\alpha^{2n+1}}{\sqrt{(2n+1)!}} |2n+1\rangle$$

$$W_{cat,odd}(X,Y) = \frac{1}{\pi(1+e^{-2\alpha^2})} \left[e^{-2(X-\alpha)^2-2Y^2} + e^{-2(X+\alpha)^2-2Y^2} - 2e^{-2X^2-2Y^2} \cos(4Y\alpha) \right].$$

C. Gerry and P. Knight. Introductory Quantum Optics. Campridge Univ. Press, 2005.

Dissipation

$$H_{osc} = \hbar\omega_0 a^+ a + f_0 \cos\Omega t (a + a^+)$$

$$\left|\alpha(t)\right\rangle = e^{\alpha(t)a^+ - \alpha^*(t)a}\left|0\right\rangle, \quad \frac{d\alpha(t)}{dt} = if_0 \cos(\omega t)$$

$$\frac{\partial\rho}{\partial t} = \frac{1}{i\hbar}[H,\rho] + \frac{\gamma}{2}(2a\rho a^+ - a^+ a\rho - \rho a^+ a)$$

$$1)\ f_0 = 0, \quad \left\langle n(t)\right\rangle = n_0 e^{-\gamma t}, \quad D(n) = n_0 e^{-2\gamma t}\left(e^{\gamma t} - 1\right)$$

$$\gamma t << 1, \quad \left\langle n(t)\right\rangle \approx n_0, \quad D(n) \approx n_0 \gamma t$$

$2)\ f_0 \neq 0,$ решения - «диссипативные когерентные состояния» $\left|\alpha_{dis}(t)\right\rangle$

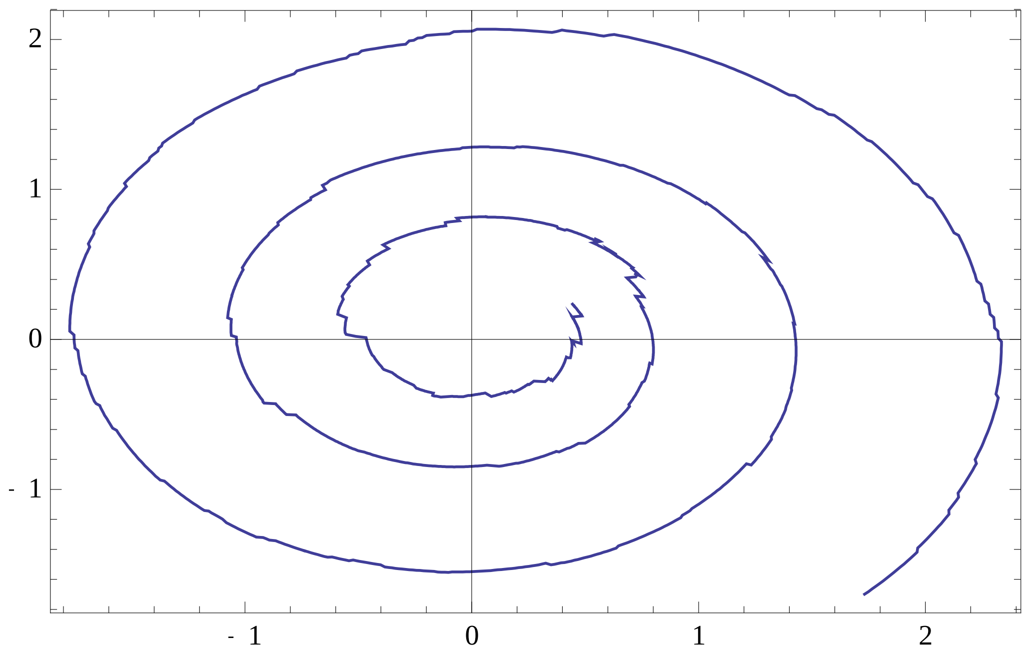
2
1
0
- 1
- 1
0
1
2

Jaynes Cummings Hamiltonian

$$H_{JC} = \frac{1}{2}\omega_{\mathrm{q}}\sigma_z + \omega a^\dagger a + g\left(a^\dagger\sigma_- + a\sigma_+\right),$$

$$C = \omega\left(\frac{1}{2}\sigma_z + a^\dagger a\right), \qquad \left[H_{JC}, C\right] = 0,$$

$$\begin{aligned} \left|+1, n\right\rangle &= \cos\theta_n \left|n\right\rangle\left|+1\right\rangle + \sin\theta_n \left|n+1\right\rangle\left|-1\right\rangle, \\ \left|-1, n\right\rangle &= -\sin\theta_n \left|n\right\rangle\left|+1\right\rangle + \cos\theta_n \left|n+1\right\rangle\left|-1\right\rangle, \end{aligned}$$

$$\theta_n = \frac{1}{2}\tan^{-1}\left(\frac{2g\sqrt{n+1}}{\omega_q - \omega}\right)$$

$$E_{\pm,n} = \omega\left(n + \frac{1}{2}\right) \pm \tfrac{1}{2}\sqrt{4g^2(n+1) + (\omega_q - \omega)^2}, E_{+,0} = \frac{\omega_q}{2}.$$

Jaynes Cummings Hamiltonian: “dressed atom” picture

$$H = \omega a^{\dagger} a + \frac{1}{2}\omega_{\mathrm{q}}\sigma_z + g\left(a^{\dagger}\sigma_- + a\sigma_+\right)$$

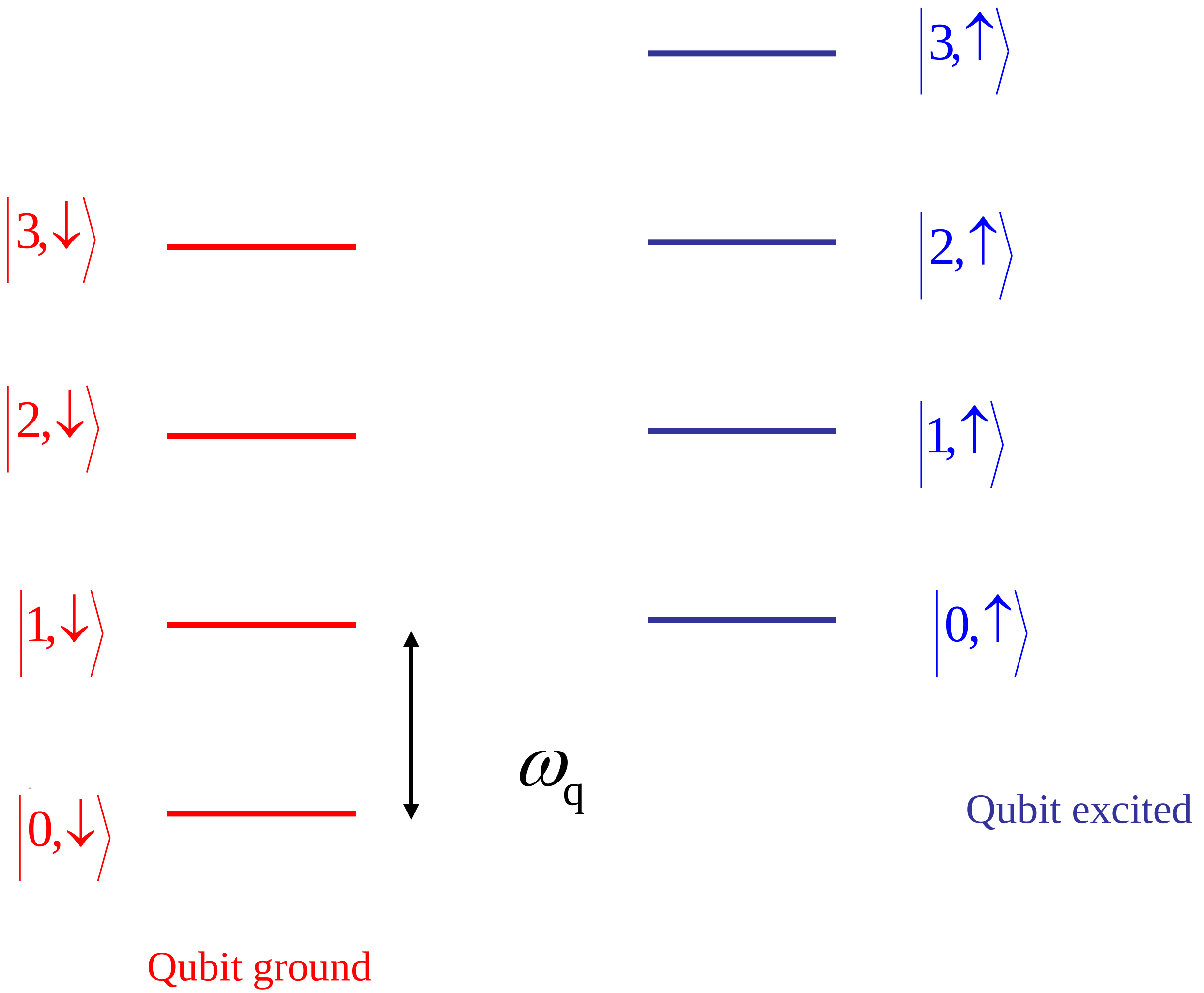

$$|\psi(0)\rangle_{\text{atom}} = C_g|g\rangle + C_e|e\rangle, \quad |\psi(0)\rangle_{\text{field}} = \sum_{n=0}^{\infty} C_n|n\rangle, \quad |\psi(0)\rangle = |\psi(0)\rangle_{\text{atom}} \otimes |\psi(0)\rangle_{\text{field}}.$$

The solution of the Schrödinger equation is now

$$|\psi(t)\rangle = \sum_{n=0}^{\infty} \{[C_e C_n \cos(\lambda t\sqrt{n+1}) - iC_g C_{n+1} \sin(\lambda t\sqrt{n+1})]\,|e\rangle$$
$$+ [-iC_e C_{n-1} \sin(\lambda t\sqrt{n}) + C_g C_n \cos(\lambda t\sqrt{n})]|g\rangle\}\,|n\rangle.$$

In general, this is an entangled state.

The atomic inversion is

$$\begin{aligned} W(t) &= \langle\psi(t)|\hat{\sigma}_3|\psi(t)\rangle \\ &= \langle\psi_e(t)|\psi_e(t)\rangle - \langle\psi_g(t)|\psi_g(t)\rangle \\ &= \sum_{n=0}^{\infty} |C_n|^2 \cos(2\lambda t\sqrt{n+1}). \end{aligned}$$

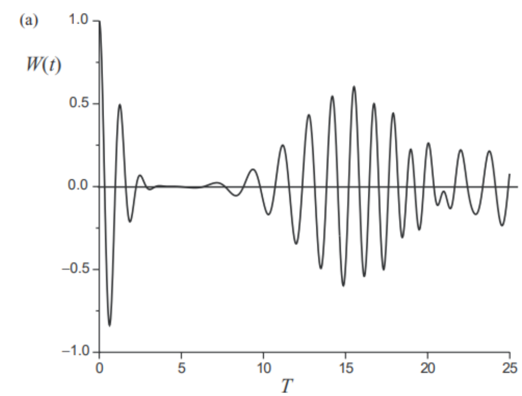

$$t_c = \frac{\sqrt{2}}{\lambda}\sqrt{\frac{\bar{n}+1}{\bar{n}}} \simeq \frac{\sqrt{2}}{\lambda}, \qquad \bar{n} \gg 1$$

C. Gerry and P. Knight. Introductory Quantum Optics. Campridge Univ. Press, 2005.

Jaynes-Cummings model: dispersive regime

$$H = \frac{\hbar\omega_q}{2}\sigma_z + \hbar a^+ a + \hbar g\left(a\sigma_+ + a^+\sigma_-\right)$$

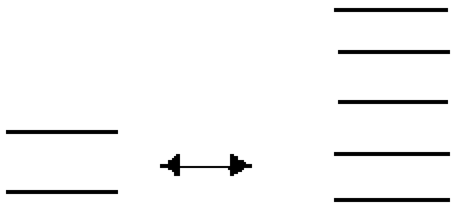

$$H_{eff} = \hbar\chi\left(\sigma_+\sigma_- + a^+ a\sigma_z\right)$$

$$\chi = \frac{g^2}{\omega_q - \omega}$$

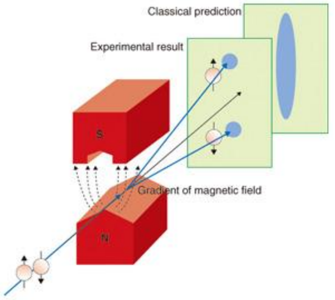

$$\left|\psi(t)\right\rangle = \hat{U}(t)\left|\psi(0)\right\rangle,$$

$$\left|\psi(0)\right\rangle = \left|g\right\rangle \otimes \left|n\right\rangle,\ \ \left|\psi(t)\right\rangle = e^{-iH_{eff}t/\hbar}\left|\psi(0)\right\rangle = e^{-i\chi nt}\left|g\right\rangle \otimes \left|n\right\rangle$$

$$\left|\psi(0)\right\rangle = \left|e\right\rangle \otimes \left|n\right\rangle,\ \ \left|\psi(t)\right\rangle = e^{i(n+1)\chi t}\left|e\right\rangle \otimes \left|n\right\rangle$$

$$\left|\psi(0)\right\rangle = \left|g\right\rangle \otimes \left|\alpha\right\rangle,\ \ \left|\psi(t)\right\rangle = \left|g\right\rangle \otimes \left|\alpha e^{i\chi t}\right\rangle$$

$$\left|\psi(0)\right\rangle = \left|e\right\rangle \otimes \left|\alpha\right\rangle,\ \ \left|\psi(t)\right\rangle = \left|e\right\rangle \otimes \left|\alpha e^{-i\chi t}\right\rangle e^{-i\chi t}$$

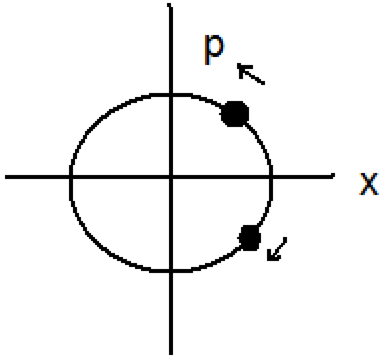

$$\left|\psi(0)\right\rangle = \frac{1}{\sqrt{2}}\left(\left|g\right\rangle + e^{i\phi}\left|e\right\rangle\right)\otimes\left|\alpha\right\rangle,\ \ \left|\psi(t)\right\rangle = \frac{1}{\sqrt{2}}\left(\left|g\right\rangle \otimes \left|\alpha e^{i\chi t}\right\rangle + e^{i\phi}e^{-i\chi t}\left|e\right\rangle \otimes \left|\alpha e^{-i\chi t}\right\rangle\right)$$

Biled, et al, "Schrödinger cat states of a 16-microgram mechanical oscillator", Science 380, 274–278 (2023)

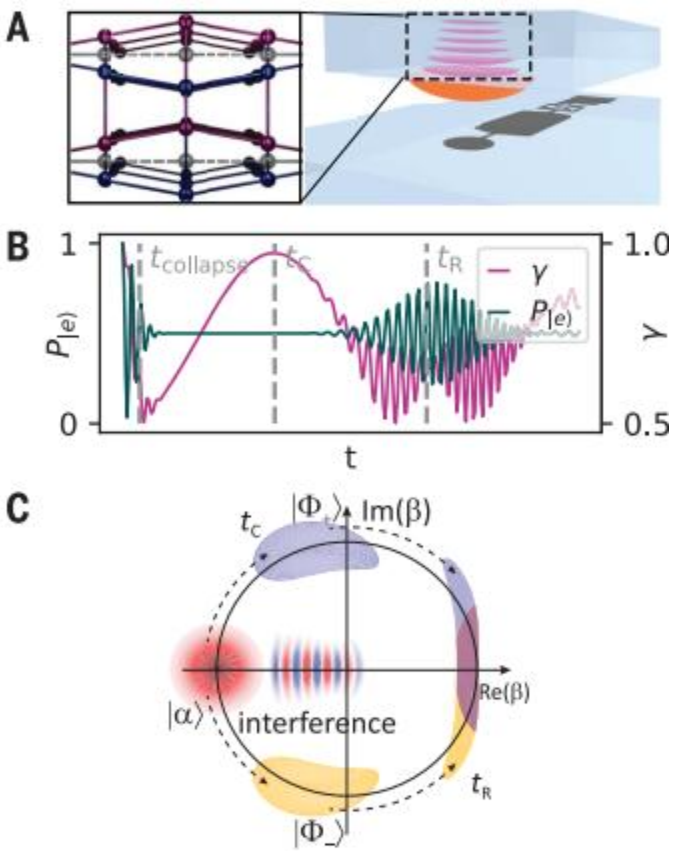

The inset shows the superposition of two opposite-phase oscillations of atoms in the crystal lattice

Simulated evolution without decoherence of the qubit $|e\rangle$ state population $P_{|e\rangle}$ and purity γ under the JC interaction when the qubit is initialized in $|-Z\rangle$ and the phonon in a coherent state.

Illustration of the evolution of an initial phonon coherent state (red circle on the left) in phase space. The blue (yellow) crescent shapes indicate the state $|\Phi_+\rangle$ ($|\Phi_-\rangle$), which is the phonon state when the qubit is initialized in $|+X\rangle$ ($|-X\rangle$). Interference fringes appear around time t_C when the qubit is prepared in a superposition of $|+X\rangle$ and $|-X\rangle$. Around the revival time t_R, the two phonon states again overlap (purple).

Collapse and revival dynamics

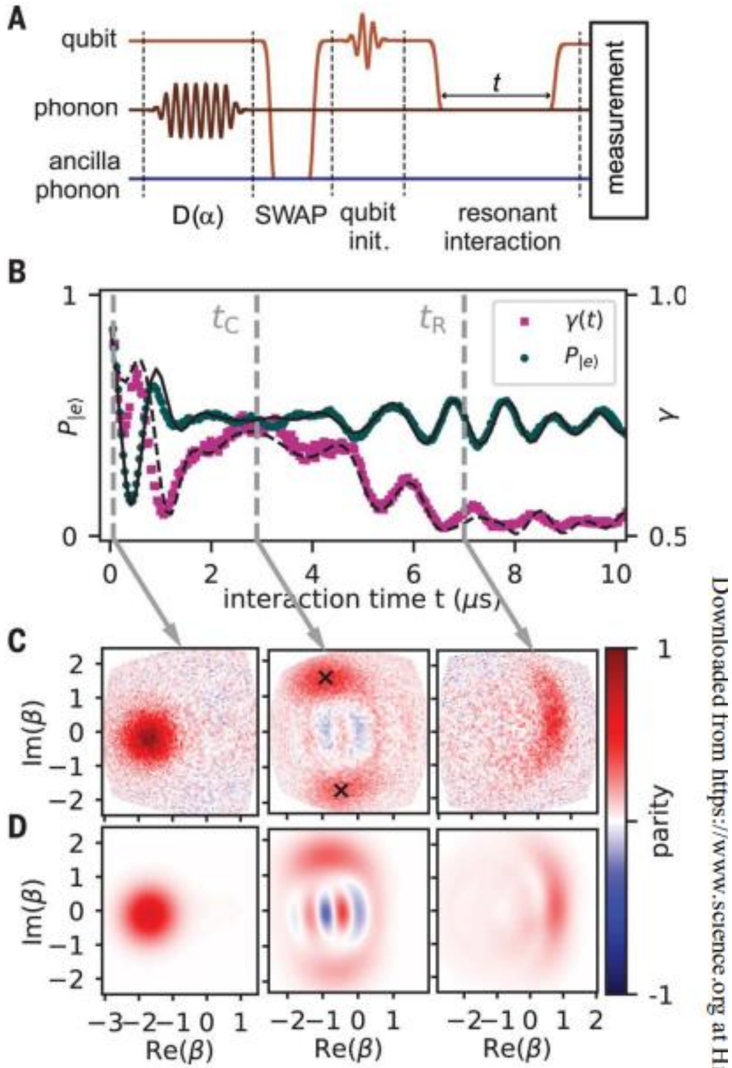

Experimental sequence for observing collapse and revivals dynamics and for preparing cat states

Measured qubit population and state purity. The solid and dashed black lines are the simulation results of the qubit population and purity, respectively. Three time points of particular interest are highlighted (dashed lines):

Measured (C) and simulated (D) Wigner functions function of the phonon state at the three time points. The black crosses indicate the positions of the two coherent states composing the fitted CSS state

$$|C\rangle = \mathcal{N}\left(|\alpha_1\rangle + e^{i\vartheta}|\alpha_2\rangle\right)$$

Cat states prepared with different displacement pulse amplitudes A.

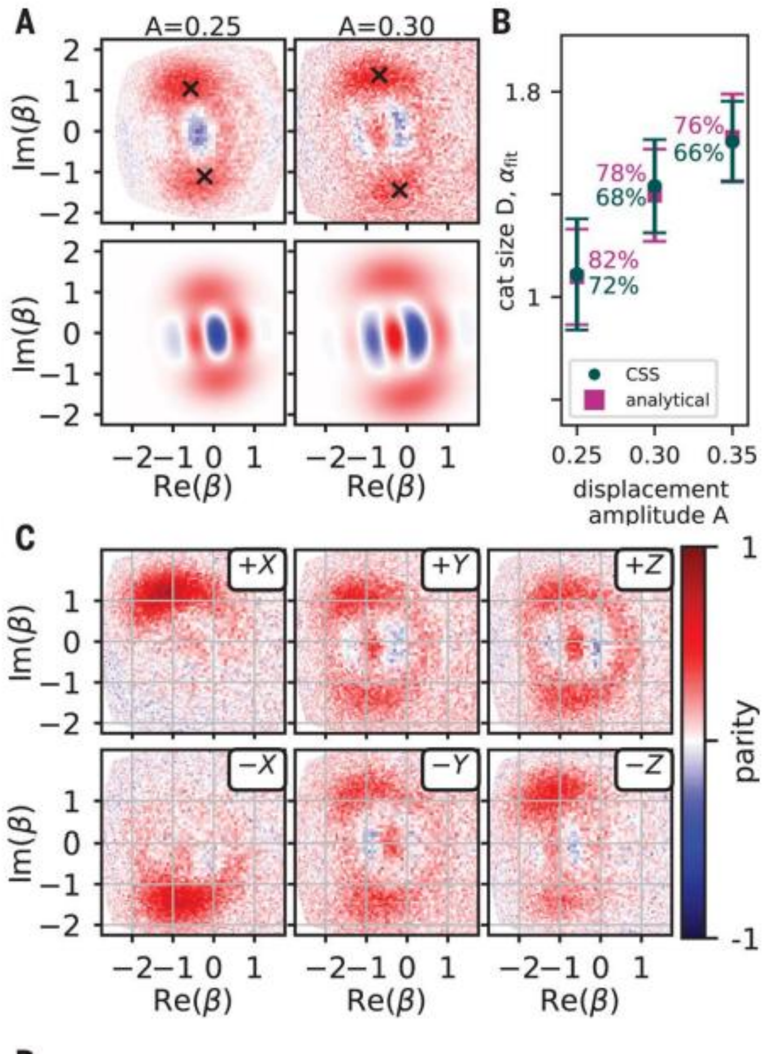

The phase space distance between the coherent state components

$$D = |\alpha_1 - \alpha_2|/2$$

$$\alpha_1 = -\alpha_2$$

$$D = |\alpha_{1,2}| = \sqrt{\bar{n}}$$

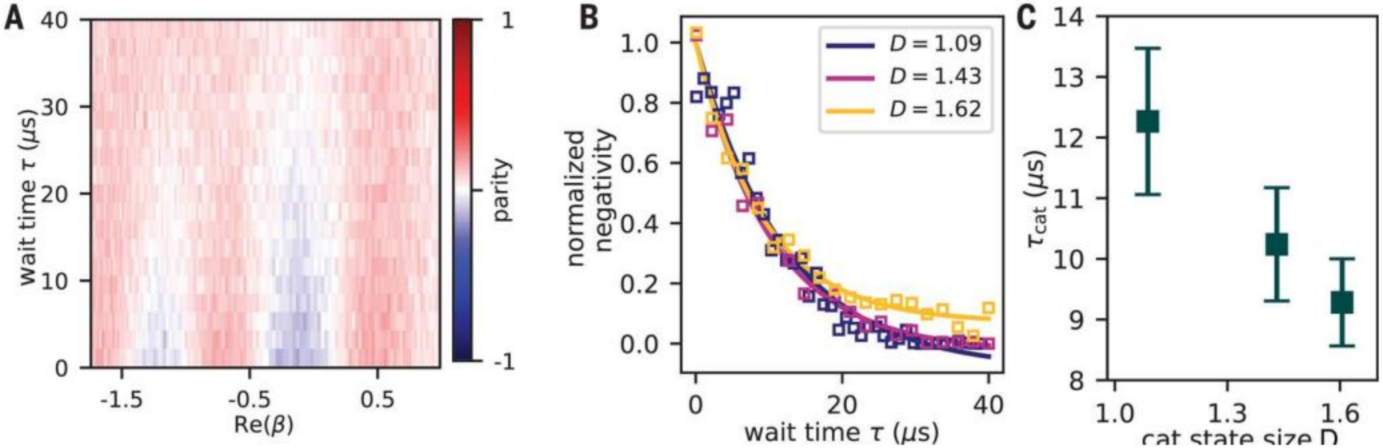

Measured 1D cuts through the interference fringes of the D = 1.43 cat state for a range of wait times between state creation and measurement.

Characteristic decay times

Summary

Results show the generation of cat states in a microgram-mass solid-state mechanical mode using the tools of cQAD.

These tests would benefit from larger-sized cat states, resonators with higher masses, and longer phonon lifetimes.

The maximum size of the cat state that we can prepare is currently limited by our device parameters, including both the qubit and phonon decoherence rates.

The latter is especially important given that, in general, the decoherence rate of the cat state is proportional to the square of the cat state size D.

Furthermore, additional improvements to the properties of qubit and phonon resonator would enable alternative cat state generation protocols that can in principle lead to states with a higher fidelity to, for example, a CSS state.